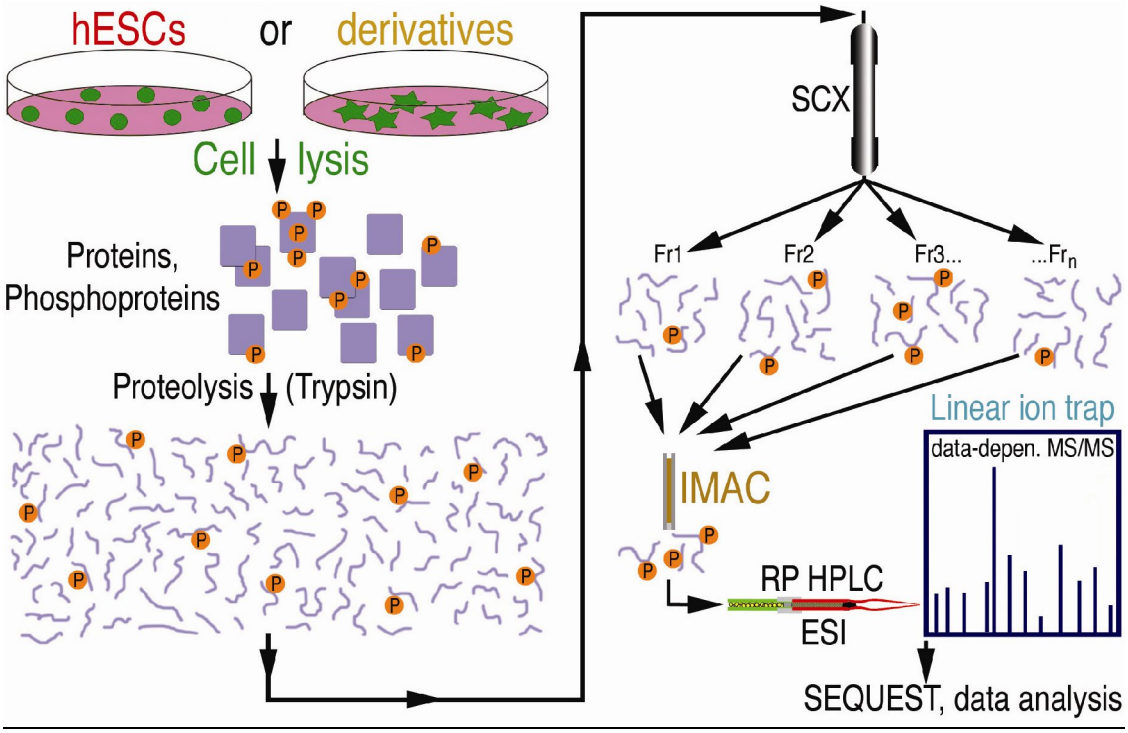

Figure S1. **Schematic Diagram of Phosphoproteomic Analysis of Undifferentiated hESCs or Derivatives of hESCs that were Non-Specifically Differentiated by the Addition of RA and the Withdrawal of bFGF.** Total proteins, including phosphorylated (represented by "P") proteins were digested and peptides were fractionated using SCX (Fr1, Fr2, Fr3… …Fr_n). Phosphorylated peptides were enriched from individual SCX fractions using automated desalt-IMAC and separated by automated, nano-flow RP HPLC coupled to ESI-MS/MS using a linear ion trap mass spectrometer. MS/MS spectra collected in the data-dependent mode (data-depen. MS/MS) were searched for peptide sequence matches using SEQUEST (Thermo Electron, Inc. (Eng et al., 1994)) and only high-confidence identifications were accepted as described in Supplementary Experimental Procedures.

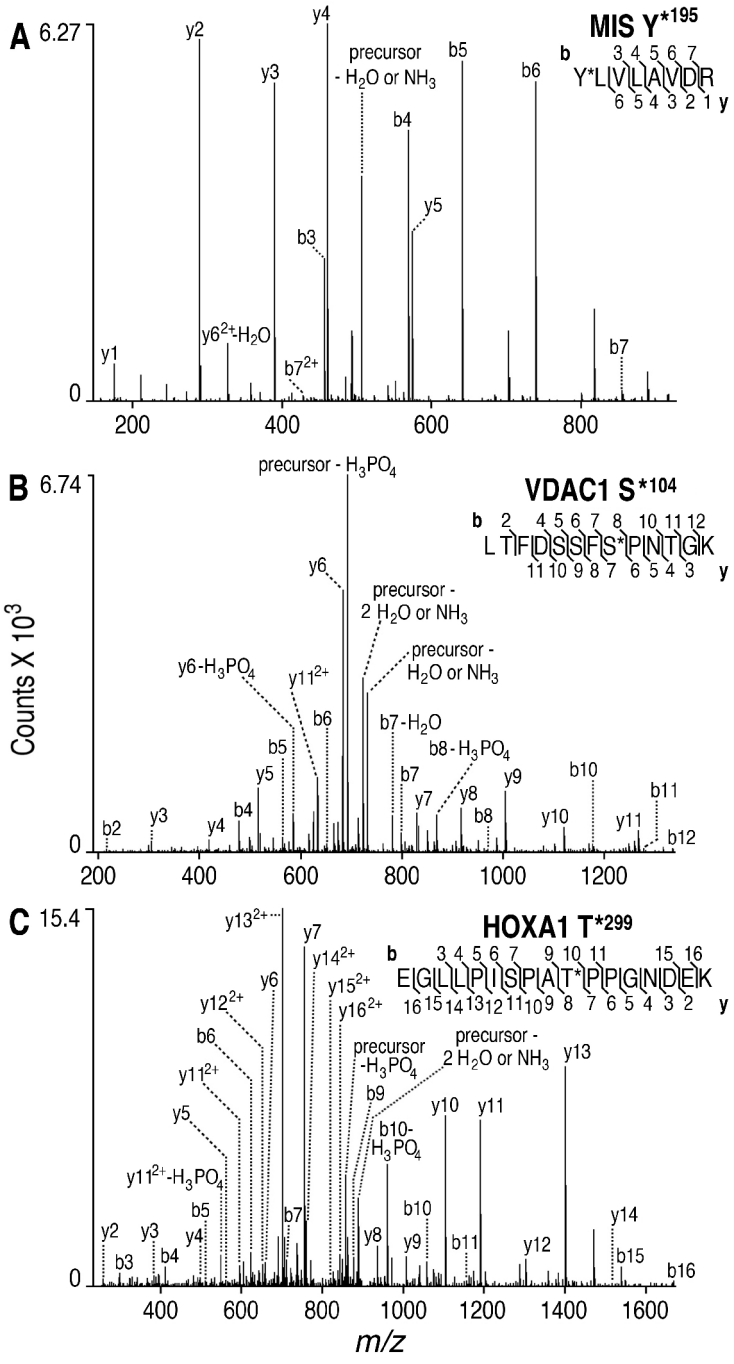

Figure S2. Representative MS/MS Spectra. Typical MS/MS spectra of phosphopeptides demonstrated Tyr phosphorylation (Y*, residue 195) of the growth factor Mullerian Inhibitory Substance (MIS; **A**), Ser phosphorylation (S*, residue 104) of voltage-dependent anion channel 1 (VDAC1; **B**) and Thr phosphorylation (T*, residue 299) of the transcription regulator HoxA1 (**C**).

The *m*/*z* (mass: charge) ratios of the b- and y- product ions and neutral loss product ions, which resulted from precursor ion fragmentation, can be seen from viewing the spectra. The b-product ions that were identified, which are listed above the one-letter codes representing the amino acid sequences, demonstrate an increasing *m*/*z* ratio when proceeding from the N-terminus toward the C-terminus of the peptides, whereas the y-product ions that were identified, which are listed below the one-letter codes representing the amino acid sequences, demonstrate an increasing *m*/*z* ratio when proceeding from the C-terminus toward the N-terminus of the peptides. Singly charged fragment ions were the dominant molecular species identified in these MS/MS spectra, and doubly charged fragment ions (shown with the superscript "2+") were also identified, but less frequently. For clarity, the numbers representing a portion of one "y ion series" is offset (**C**). The sequence coverage that was obtained via these MS/MS spectra allowed unambiguous identification of the peptide sequences and phosphorylation sites. Consistent with the known characteristics of MS/MS spectra of phosphopeptides (Ficarro et al., 2002; Thingholm et al., 2008), no detectable neutral loss of H_3PO_4 (phosphoric acid) was observed from this Tyr phosporylated peptide (**A**) (some Tyr-phosphorylated peptides demonstrate neutral loss, including HPO_3), abundant neutral loss of H_3PO_4 was observed from this Ser phosporylated peptide (**B**), and intermediate amounts of neutral loss of H_3PO_4 was observed from this Thr phosporylated peptide (**C**). Although each phosphopeptide displays a unique fragmentation pattern, these neutral loss trends were typical of the MS/MS spectra that were used to identify the phosphopeptides in this study, and helped to confirm the phosphopeptide identifications.

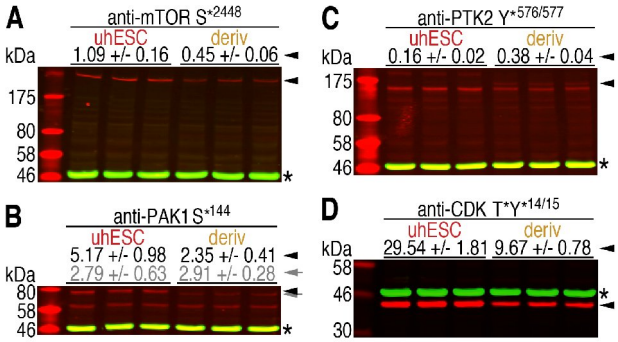

FIGURE S3. Semi-Quantitative Western Blot Analysis, using Antibodies that Recognize Specific Protein Phosphorylation Sites, Supported Phosphoproteomic Results using MDLC-MS/MS. Proteins were prepared from undifferentiated hESCs (**"uhESC"**) or their differentiated derivatives (**"deriv"**), and Western blot analysis, including normalized, integrated intensities of the bands, were performed (**Supplementary Experimental Procedures**). Protein molecular mass standards, in kilodaltons (kDa) are shown **(A-D)**. Triplicate lanes contained proteins from either undifferentiated hESCs or derivative cell populations. Each experimental antibody recognizes protein phosphorylation site(s) identified in the MDLC-MS/MS analysis reported in this paper. Integrated intensities of experimental bands were normalized by dividing their integrated intensities by the integrated intensity of the glyceralde-3-phosphate dehydrogenase (GAPDH) loading control **(*)**. Normalized integrated mean intensities (percentage of the GAPDH control), +/- the standard deviation is shown above the blots. Arrowheads mark specific experimental bands recognized by the antibodies and their normalized, integrated intensity **(A-D)**. The arrow **(B)** marks a band putatively containing phospho-PAK2, also recognized by the antibody recognizing phospho-PAK1 (see **Supplementary Experimental Procedures**), and its normalized, integrated intensity. The target protein phosphorylation site of each antibody is indicated at the top of each panel, and were mTOR (official symbol FRAP1) phosphorylated on Ser2448 **(A)**; PAK1 phosphorylated on Ser144 **(B)**; PTK2 phosphorylated on Tyr576/Tyr577 **(C)**; and CDK1/2/3/5 phosphorylated on Thr14 and Tyr15 **(D)**.

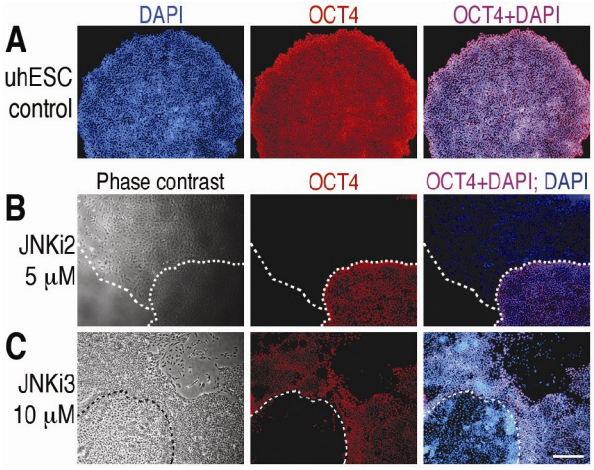

Figure S4. Consistent with Phosphoproteomic and Pathway Analyses, Treatment with JNK Inhibitors Resulted in Differentiation of hESCs. (**A**) An example of the undifferentiated control colonies ("uhESC") that were stained to detect nuclear fluorescence from DAPI (blue), stained to detect OCT4 (red), and the two images merged to reveal overlap of OCT4 and DAPI staining (magenta). (**B, C**) Images were from phase contrast microscopy (left column), immunostaining for OCT4 (middle column, red) or merged OCT4 and DAPI staining (right column: Magenta, or DAPI alone, visualized as blue in differentiated areas of the colonies with minimal OCT4 staining). Concentrations of JNK inhibitor II (JNKi2; **B**) or JNK inhibitor III (JNKi3; **C**) are indicated beside the rows. Dotted curves mark approximate boundaries between more and less extensive differentiation. All photomicrographs were at the same magnification, and the scale bar (bottom right) represents 50 μM.

SUPPLEMENTARY EXPERIMENTAL PROCEDURES

Cell culture

hESCs were recovered from frozen stocks in the presence of X-ray irradiated mouse embryonic fibroblast (MEF) line CF1 feeder cells in DMEM/F-12 medium supplemented with 20% Knock-Out Serum Replacement, 2 mM L-Glutamine, 1.1 mM 2-mercaptoethanol, 1 mM non-essential amino acids and 8 ng/ml bFGF (Invitrogen Inc., Carlsbad, CA). Cells were passaged at the ratio of 1:5 every 5 or 6 days with 1 mg/ml Collagenase Type IV (Invitrogen). Cell cultures used in phosphoproteomic analyses were expanded in Matrigel coated culture plates, under feeder free conditions, in CM containing 8 ng/ml of bFGF as described previously (Xu et al., 2001). Differentiation of hESCs that were used for phosphoproteomic analyses was in the presence of 5 μM RA and the absence of exogenous bFGF for the final 4 d of culture.

For feeder free culture in CDM, hESCs were grown in Matrigel-coated tissue culture plates in N2/B27-CDM (Yao et al., 2006), and passaged using Dispage (1mg/mL, Invitrogen). The N2/B27-CDM is defined as DMEM/F-12 with 1X N2 supplements, 1X B27 supplements, 2 mM L-Glutamine, 0.11 mM 2-mercaptoethanol, 1 mM non-essential amino acids, and 0.5 mg/ml BSA (fraction V).

Preparation of proteins and peptides

For each phosphoproteomic analysis, ca. 2 X 10^7 cells were cultured under feeder-free conditions in CM at ca. 50% confluence as either undifferentiated hESCs or differentiated derivatives as described above. The procedures were performed separately on independent (biological replicate) cultures.

Culture media was aspirated, plates were immediately placed on ice, cells were rinsed with ice cold Dulbecco's phosphate buffered saline (PBS) and lysed in 3 ml of ice-cold lysis buffer (Brill et al., 2004) per ca. 1 X 10^7 cells in a 150 mm diameter culture plate. Lysates were

agitated on ice for 30 min at ca. 1 Hz and centrifuged for 20 min at 15,000 g, 2 °C. Supernatants were centrifuged again, $(NH_4)_2SO_4$ crystals were added to the supernatant at 608 mg/ml, and mixtures were placed on a rotator wheel at ca. 1 Hz, 4 °C overnight and centrifuged for 20 min at 15,000 g, 2 °C. Supernatants were discarded and protein pellets were stored at -75 °C.

Protein pellets were rinsed with ice-cold Dulbecco's PBS containing 608 mg/ml $(NH_4)_2SO_4$, 100 nM Calyculin A (Cell Signaling Technology Inc., Beverly, MA) and Phosphatase Inhibitor Cocktails I & II (Sigma Chemical Co., St. Louis, MO) at a 1:100 dilution. Tubes were centrifuged at 15,000 g, 20 min, 2 °C, supernatants were discarded, and pellets were solublized in 100 mM NH_4HCO_3 buffer, pH 8.3 containing 8 M urea, 100 nM Calyculin A and phosphatase inhibitor cocktails I and II (1:100 dilution). Residual phenol red from the culture medium, and potentially other contaminants were depleted using PD-10 desalting columns according to the manufacturer's instructions (GE Healthcare), in the presence of Calyculin A and phosphatase inhibitor Cocktails I and II, at the concentrations described above. Protein concentrations were estimated using Bio-Rad Protein Assays (Bio-Rad, Inc., Hercules, CA). Proteins were diluted 1:1 v/v with 80% water/20% glycerol and stored at -75 °C.

Protein (1 mg) was digested by adding 0.1 vol. of 1 M NH_4HCO_3 buffer, pH 8.3 and 100 μg of modified sequencing grade trypsin (Promega Inc., Madison, WI) and incubating overnight at 37 °C. For reduction of Cys residues, dithiothreitol was added to 10 mM and the mixture incubated 30 min at 37 °C. Alkylation (carboxamidomethylation) was with 20 mM IAA for 45 min at room temperature in the dark. An equal volume of 0.1 M NH_4HCO_3 buffer, pH 8.3 and 100 μg of modified sequencing grade trypsin was added and incubated overnight at 37 °C. The resulting peptides were desalted with Sep-Pak® C18 Cartridges (Waters), liquid removed in a Speed Vac (Thermo Fisher Scientific, Inc., San Jose, CA) until ca. 50 μl remained, and stored at -75 °C.

Multidimensional liquid chromatography and phosphopeptide identification

Peptides were fractionated using a SCX procedure similar to a previous report (Gruhler et al., 2005). 250 µl of SCX solvent A was added to the peptides (solvent A = 5 mM KH_2PO_4 pH 2.7/25% acetonitrile; solvent B = solvent A containing 500 mM KCl). A polysulfoethyl A column, 200 X 2.1 mm, containing 5 µm beads, 200 Å pore size (PolyLC, Inc., Columbia, MD) was used at a flow rate of 200 µl/min. The gradient was 0% B - 15% B in 5 min, 15% B - 65% B in the next 20 min, 65% B - 100% B in the next 5 min, then 100% B - 0% B in the final 5 min. Thirty x 200 µl fractions were collected, dried in a speed vac, each SCX fraction was re-suspended in 50 µl of 0.1% acetic acid, and stored at -75 °C. Enrichment of phosphopeptides from SCX fractions (25 of the 50 µl per enrichment) was by automated RP desalt-Fe^{3+}-IMAC (Brill et al., 2004; Ficarro et al., 2005; Posewitz and Tempst, 1999). Peptides were eluted from IMAC to RP media and separated by nanoflow-RP HPLC coupled to ESI-MS/MS. Desalt-IMAC, RP HPLC and ESI were on an automated system described previously (Ficarro et al., 2005) coupled to an LTQ linear ion trap mass spectrometer (no FT-ICR or Orbitrap; Thermo Fisher Scientific). The mass spectrometer, in the positive ion mode, recorded cycles of one ESI mass spectrum followed by MS/MS scans of the 5 most abundant precursor ions in each ESI mass spectrum, fragmented using collision-induced dissociation. Dynamic exclusion specified a repeat count of 1 and exclusion duration of 30 s. MS/MS spectra were matched to amino acid sequences in the national center for biotechnology information (NCBI) non-redundant human protein database (version from 4 August 2004) using SEQUEST (Eng et al., 1994) (Bioworks Rev. 3.1 SR_1; Thermo Fisher Scientific). Searches specified differential modifications of +80.0 Da to Ser, Thr, and Tyr residues (phosphorylation) and +16.0 Da to Met residues (oxidation), static modification of +57.0 Da to Cys (carboxamidomethylation), tryptic specificity and a maximum of 2 missed cleavages. Precursor ion mass tolerances were 1.5 Da and fragment ion tolerances were 0.5 Da. All reported

phosphopeptide identifications, which all had SEQUEST Xcorr scores $\geq$2.5 for 3^+, $\geq$2.0 for 2^+ and $\geq$1.5 for 1^+ peptides, were verified by manual interpretation of MS/MS spectra as described previously (Bernstein et al., 2008; Brill et al., 2004; Ficarro et al., 2005). Most SEQUEST Xcorr scores of accepted peptide identifications were substantially higher than these thresholds, and are shown for all accepted peptide identifications (**Tables S3A-S5B**). Phosphopeptide identifications are reported following "Publication Guidelines for the Analysis and Documentation of Peptide and Protein Identifications" from the Molecular and Cellular Proteomics website (http://www.mcponline.org/misc/ParisReport_Final.shtml).

Some phosphopeptides containing adjacent Ser, Thr and/or Tyr residues had SEQUEST delta CN values that were relatively low, and the exact phosphorylated residue was sometimes ambiguous, in agreement with other reports (Beausoleil et al., 2006; Bodenmiller et al., 2007). Delta CN values of all accepted peptide identifications are shown in **Tables 3SA-S5B**, and typically the higher delta CN values denote unambiguous sites of phosphorylation. Phosphorylation site ambiguities are also indicated in **Tables S3A-S5B** with parentheses that were manually inserted to indicate the range of residues to which the phosphate group could be localized. Some phosphorylation sites could be identified with high confidence in spite of relatively low delta CN values because the same site was identified two or usually more times, and most phosphorylation sites were identified with high confidence due to thorough peptide sequence coverage by the MS/MS fragment ions. In spite of ambiguity of some phosphorylation sites, phosphopeptide identifications were confident. Ambiguous sites will not negatively impact pathway analyses and cellular assays, because the unit that was focused upon was the phosphoprotein for these follow-up analyses.

Semi-quantitative assessment of phosphopeptide abundance from MS/MS data

Extracted ion chromatogram (XIC) peak areas of phosphopeptides were measured using Xcalibur v.2.0 software (Thermo Fisher Scientific). If a phosphopeptide was identified in 2 or more SCX

fractions from an individual analysis, the XIC peak areas for that peptide were summed (see **Figure S1 for a schematic overview of the analyses**). XIC peak areas were normalized among all 4 analyses by deriving a normalization coefficient for each analysis. Normalization coefficients were the ratios, among all 4 analyses, of the composite number of raw counts per analysis, in which the raw counts were derived from a collection of 20 randomly chosen phosphopeptides, each of which was identified in each of the 4 analyses. Each of these 20 peptides was identified *via* validated SEQUEST searches of the MS/MS data, as described above, and its XIC peak area was quantified in each of the 4 analyses. Subsequently, the number of raw counts for individual phosphopeptides in each analysis was divided by the normalization coefficient for that same analysis to obtain normalized peak areas for individual phosphopeptides (**Tables S1 and S2**). The analysis containing the fewest normalized counts for an individual phosphopeptide was set to a relative abundance of 1.00 for that phosphopeptide (**Tables S1 and S2**).

For a randomly chosen sample of phosphopeptides identified in only undifferentiated hESCs or differentiated hESC derivatives, the peak areas from XICs were quantified and normalized as described above, for analyses in which the identifications were made. For the analyses lacking the identification of a phosphopeptide, raw MS/MS data was exhaustively searched for a candidate precursor ion of the phosphopeptide, potentially present but not identified *via* SEQUEST searches, by aligning XIC peaks from IMAC enrichments of SCX fractions followed by LC-MS/MS from analyses lacking the identified phosphopeptide with the XIC peaks from analyses containing the phosphopeptide identification (**Table S2**; see **Figure S1 for a schematic overview of the analyses**). XIC peak alignment was facilitated by the high degree of reproducibility of the automated multidimensional LC-MS/MS system that was used (Ficarro et al., 2005). A precursor ion XIC peak with a similar retention time and an m/z within ± 0.5 suggested a candidate precursor ion of the phosphopeptide in question. In the unusual instances when a candidate precursor was found, an MS/MS scan of the candidate precursor was

exhaustively sought to confirm or refute the identity of the ion as the phosphopeptide whose identification was potentially missed by the MS/MS data generation and SEQUEST searches. Most of the candidate precursors were clearly different ions, but in the rare instances in which a phosphopeptide was detectable via a poor quality MS/MS spectrum, but its identification had been missed by SEQUEST searches (shown in **Table S2**; methodology for SEQUEST-based identifications described above), its XIC peak area was quantified as described above.

Recognizing that phosphopeptide identifications were unlikely to be comprehensive, but that there was a correlation between phosphopeptide identification and normalized abundance of the phosphopeptide (as explained in the main text and shown in **Figure S3** as well as **Table S2**), phosphoproteins were conservatively classified as containing more phosphorylation site identifications in undifferentiated hESC populations or differentiated hESC derivative populations if they were identified only in undifferentiated or differentiated cell populations (from the 2 combined biological replicates of each cell population), or if there was a 3-fold or greater number of phosphopeptide identifications on the protein in the population that contained more phosphorylation site identifications. All other phosphoproteins were considered to contain a similar number of phosphorylation site identifications between undifferentiated hESCs and their differentiated derivatives. Phosphopeptides that were identified in 2 or more SCX fractions (see **Figure S1**) from an individual analysis were counted as having been identified twice, reflecting their relatively high abundance, in order to suggest whether the phosphoprotein from which they were derived should be considered as containing more phosphorylation identifications in the undifferentiated or differentiated cell populations.

Use of motif-x software (http://motif-x.med.harvard.edu/) did not reveal clear differences in phosphorylated protein sequence motifs between undifferentiated hESCs, differentiated derivatives, or shared phosphoproteins. Similarly, no clear differences were revealed in the protein kinases predicted to catalyze protein phosphorylation in undifferentiated hESCs or their differentiated derivatives, on the basis of the phosphopeptides identified in undifferentiated

hESCs, those identified in the differentiated derivatives, or those identified in both cell populations.

Semi-quantitative assessment of phosphorylation site abundance using Western blot analysis

hESCs and their differentiated derivatives were cultured in 2 pairs of biological replicate cultures (undifferentiated and differentiated cells comprising each pair) in CM as described above. Cells were rinsed with ice-cold PBS, lysed in buffer containing 50mM Tris-HCl, pH 7.4, 150 mM NaCl, 0.25% deoxycholic acid, 1.0 % NP-40, 1.0 mM EDTA, as well as protease and phosphatase inhibitor cocktail used at the concentration recommended by the manufacturer (Thermo-Fisher Scientific/Pierce, Rockford, IL). Lysates were centrifuged at 16,000 g for 10 min at 4 °C and the protein concentration of the supernatants were estimated using the Bio-Rad Protein Assay. Proteins were incubated at 70 °C in lithium dodecyl sulfate (LDS) loading buffer (26.5 mM Tris-HCl, 35.25 mM Tris-Base, 0.5 % LDS, 2.5 % Glycerol, 0.13 mM EDTA, 55 µM Coomassie Brilliant Blue G250, 44 µM Phenol Red, pH 8.5) for 10 min. Circa 25 µg protein was loaded per lane on 4-12% Bis-Tris gels (Invitrogen) and run under reducing and denaturing conditions, according to the manufacturer, at 200 V for 30 min. A minimum of triplicate lanes was run for each protein preparation (4 preparations were used; 2 pairs of preparations from undifferentiated and differentiated cells) and each experimental antibody used. A broad range pre-stained protein standard (New England Biolabs, Ipswitch, MA) was included for estimation of apparent molecular masses. Proteins were transferred from gels to polyvinylidene fluoride (PVDF) membranes and blocked overnight in 5.0 % non-fat dry milk in Tris buffered saline + 0.1% Tween-20 (NFDM/TTBS) at 4 °C with gentle shaking. Primary antibodies, all recognizing protein phosphorylation sites identified via MDLC-MS/MS, were anti-HSP27 S^{*82} (i.e. recognizing HSP27 phosphorylated on serine residue 82), catalog number (cat#) 2406; anti-JUN S^{*63}, cat# 2361; anti-LMNA (lamin A/C) S^{*22}, cat# 2026; anti-PRKAA2 (AMPK alpha) T^{*172},

cat# 2535; anti-PTK2 (FAK) Y*$^{576/577}$, cat# 3281; anti-RB1 S*^{795}, cat# 9301; anti-mTOR (FRAP1) S*^{2448}, cat# 2971; anti-PAK1/2 S*$^{144/141}$, cat# 2606 (Cell Signaling Technology, Inc., (CST) Beverly, MA) and anti-CDK T*Y*^{14,15}, cat# sc-28435-R (Santa Cruz Biotechnology, Inc., Santa Cruz, CA). The correct bands, recognized by all of the CST antibodies that were used, are shown on the CST website. Although similar data is not shown for the anti-CDK2 T*Y*^{14,15} antibody, a product citation is available on the Santa Cruz Biotechnology website, and the antibody recognized a band with the expected apparent molecular mass in Western blots (**Figure S3D**). Primary antibodies were diluted 1:1,000 in 5.0 % bovine serum albumin (BSA)/TTBS and membranes incubated overnight at 4 °C with gentle shaking. As a control for protein loading, mouse anti-GAPDH (MAB374, Millipore, Inc., Temecula, CA), at a 1:1,000 dilution, was included during incubation of the experimental primary antibodies (above). Membranes were then washed 3 X 5 min in TTBS at room temp. Fluorophore-conjugated anti-rabbit 680 (Invitrogen) and anti-Mouse 800 (Rockland, Inc., Gilbertsville, PA) were diluted 1:5,000 in 5.0% BSA/TTBS and membranes were incubated for one hour at room temp with gentle shaking. After washing 3 X 5 min in TTBS at room temp, membranes were imaged using an Odyssey Imager (LiCor, Inc., Lincoln, NE) at medium (169 µM) resolution with intensity settings of 5 for both the 700 and 800 nm channels.

Bands were quantified using Odyssey 3.0 software (LiCor). Individual bands that matched the expected relative molecular mass were identified in all cases. The integrated intensity was determined for the experimental band and the GAPDH loading control band in the same individual lanes. Per the recommendation of the manufacturer, background subtraction was set to the average integrated intensity 3 pixels above and below the bands whose intensities were integrated, except for phosphorylated Tyr576/577 of PTK2. Due to the presence of a band with a slightly higher mobility than the band containing phosphorylated PTK2, background subtraction was set to the average integrated intensity 2 pixels to each side of the bands, for this site only, also per the manufacturer's recommendation. The integrated intensity value for the experimental

band was divided by the integrated intensity value of the loading control (GAPDH) band from the same lane to obtain the normalized relative abundance of the experimental bands (shown as mean percentages +/- standard deviations in **Figure S3**).

Analysis of phosphoprotein identity, subcellular locations, families and pathways

Because SEQUEST-derived phosphopeptide identifications were accompanied by NCBI gi numbers, which sometimes created ambiguity about the identity of the phosphoprotein from which the phosphopeptide was derived, NCBI gi numbers were converted to official NCBI Gene ID numbers, using in-house software, which minimized ambiguity of the identity of the phosphoprotein from which the phosphopeptide was derived. Phosphopeptides were grouped together on the basis of the ID of the gene encoding the phosphoprotein from which they were derived, and the low percentage of phosphopeptides for which a Gene ID could not be obtained (**Tables S3B, S4B and S5B**), including a manual search of NCBI databases, were grouped in alphabetical order based on the protein name associated with the NCBI gi number. All identifications are listed in **Tables S3A-S5B**.

Ingenuity Systems Inc. (Redwood City, CA; http://www.ingenuity.com/) software, v. 3.0, was used to initially suggest gene products' (phosphoproteins') subcellular location and protein category (**Tables S3A-S7**). All subcellular locations and protein categories suggested by Ingenuity Pathway Analysis (IPA) were manually examined using NCBI Entrez Gene websites, by clicking on the link for the official symbol of the gene encoding the phosphoprotein, which opened linked websites that revealed extensive information about the gene and its product, including the NCBI Gene References into Function (Gene RIF tool) and GeneOntology. Examination of this information was performed for all categorized proteins. Examination of the peer-reviewed literature that was accessed through links in the Gene RIF tool was also performed for each phosphoprotein containing any RIF citations. During these examinations, any previously introduced errors from IPA were corrected using the information provided by the Gene RIF tool,

the peer reviewed literature cited therein, and by GeneOntology. Subcellular location and simplified protein category/prominent function is listed for all phosphoproteins, for which information was available, in **Tables S3A-S7**. To identify canonical and metabolic pathways and their phosphoprotein members, IPA v. 3.0, GeneGo Metacore Analysis (http://www.genego.com/), pathways accessed through Entrez Gene links (primarily KEGG pathways), further manual inspection using NCBI websites described above, and examination of the peer-reviewed literature, including some of the articles cited in the main text, was used.

Cell treatments and immunostaining

EGFR inhibitor cyclopropanecarboxylic acid, KDR inhibitor II ((*Z*)-5-Bromo-3-(4,5,6,7-tetrahydro-1*H*-indol-2-ylmethylene)-1,3-dihydroindol-2-one), JNK inhibitor II (SP600125) and JNK inhibitor III (cell-permeable peptide; Ac-Tyr-Gly-Arg-Lys-Lys-Arg-Arg-Gln-Arg-Arg-Arg-gaba-Ile-Leu-Lys-Gln-Ser-Met-Thr-Leu-Asn-Leu-Ala-Asp-Pro-Val-Gly-Ser-Leu-Lys-Pro-His-Leu-Arg-Ala-Lys-Asn-NH_2) were from EMD Biosciences, Inc. (San Diego, CA). PDGFR inhibitor (Gleevec; clinically approved cancer chemotherapeutic agent) was obtained from the Genomics Institute of the Novartis Research Foundation, Inc. (San Diego, CA). All inhibitors were dissolved in DMSO and the final concentrations in the culture media are indicated in the text and figures, and were used to treat cells for 4 days. Each experiment using an inhibitor was performed three times, using independent cultures in each experiment. Untreated controls and vehicle-only controls, treated with DMSO lacking inhibitor, were included with each experiment. Recombinant EGF, VEGF-AA and PDGF-AA were from R&D Systems, Inc. (Minneapolis, MN). Several doses of EGF or VEGF-AA were used in cultures in the absence of bFGF, or in the presence of various doses of bFGF. 10 ng/ml of PDGF-AA was used together with 4 ng/ml of bFGF in the cultures in CDM for >15 passages, with the cells remaining in the undifferentiated state and showing no signs of differentiation beyond low levels (described in the main text and

shown in the figures). Cultures were maintained in the presence of PDGF-AA in four independent (biological replicate) experiments.

For OCT4 and SSEA-4 immunostaining and DAPI staining, hESC colonies were fixed and stained using standard procedures. Monoclonal mouse anti-OCT4 and anti-SSEA-4 (Chemicon Inc., Temecula, CA) were used at a 1:100 dilution. Secondary antibodies, (Jackson ImmunoResearch Laboratories, West Grove, PA) were Cy2™-conjugated rabbit anti-mouse IgM, μ chain specific, at a 1:200 dilution and Cy3™-conjugated rabbit anti-mouse IgG, Fcγ fragment specific, at a 1:500 dilution.

Reverse transcription-polymerase chain reaction (RT-PCR)

Cells were harvested using Trypsin, washed with PBS and mRNA was isolated using RNeasy mini-prep kits (QIAgen Inc., Chatsworth, CA). Complementary (c) DNA was synthesized with the SuperScript™ first-strand synthesis system kit (Invitrogen). The following primer pairs were used to amplify the following cDNAs; all sequences were from human: *OCT4*: 5'-GAGCAAAACCCGGAGGAGT-3' (forward) and 5'-TTCTCTTTCGGGCCTGCAC-3' (reverse); *NANOG*: 5'-GCTTGCCTTGCTTTGAAGCA-3' (forward) and 5'-TTCTTGACTGGGACCTTGTC-3' (reverse); *GAPDH*: 5'-AGCCACATCGCTCAGACACC-3' (forward) and 5'-GTACTCAGCGGCCAGCATCG-3' (reverse). PCR reactions were under the following conditions: 180 sec at 94 °C; then 35 cycles of 30 sec at 94 °C, 30 sec at 55 °C and 60 sec at 72 °C, and reactions were completed by 600 sec at 72 °C.

Fluorescence Activated Cell Sorting (FACS)

Cultured cells were trypsinzed, re-suspended and incubated for 30 min at 4 °C with mouse monoclonal anti-SSEA-4 or anti-TRA-1-60 antibodies (Chemicon) diluted 1:100 in PBS containing 0.4% fetal bovine serum. Cells were washed twice with PBS, and incubated for 30 min

at 4 °C with Cy3™-conjugated rabbit anti-mouse IgG, Fcγ fragment specific, at a 1:500 dilution in PBS containing 0.4% fetal bovine serum. Cells were washed three times with PBS, data was collected using a BD LSRII flow cytometry system (BD Biosciences Inc., San Jose, CA), and data was analyzed using FLOWJO software (TreeStar, Inc., Ashland, OR).

REFERENCES

Beausoleil, S. A., Villen, J., Gerber, S. A., Rush, J., and Gygi, S. P. (2006). A probability-based approach for high-throughput protein phosphorylation analysis and site localization. Nat Biotechnol *24*, 1285-1292.

Bernstein, E., Muratore-Schroeder, T. L., Diaz, R. L., Chow, J. C., Changolkar, L. N., Shabanowitz, J., Heard, E., Pehrson, J. R., Hunt, D. F., and Allis, C. D. (2008). A phosphorylated subpopulation of the histone variant macroH2A1 is excluded from the inactive X chromosome and enriched during mitosis. Proc Natl Acad Sci U S A *105*, 1533-1538.

Bodenmiller, B., Mueller, L. N., Mueller, M., Domon, B., and Aebersold, R. (2007). Reproducible isolation of distinct, overlapping segments of the phosphoproteome. Nat Methods *4*, 231-237.

Brill, L. M., Salomon, A. R., Ficarro, S. B., Mukherji, M., Stettler-Gill, M., and Peters, E. C. (2004). Robust phosphoproteomic profiling of tyrosine phosphorylation sites from human T cells using immobilized metal affinity chromatography and tandem mass spectrometry. Anal Chem *76*, 2763-2772.

Eng, J., McCormack, A., and Yates, J. R. (1994). An Approach to Correlate Tandem Mass Spectral Data of Peptides with Amino Acid Sequences in a Protein Database. J Am Soc Mass Spec *5*, 976-989.

Ficarro, S. B., McCleland, M. L., Stukenberg, P. T., Burke, D. J., Ross, M. M., Shabanowitz, J., Hunt, D. F., and White, F. M. (2002). Phosphoproteome analysis by mass spectrometry and its application to Saccharomyces cerevisiae. Nat Biotechnol *20*, 301-305.

Ficarro, S. B., Salomon, A. R., Brill, L. M., Mason, D. E., Stettler-Gill, M., Brock, A., and Peters, E. C. (2005). Automated immobilized metal affinity chromatography/nano-liquid chromatography/electrospray ionization mass spectrometry platform for profiling protein phosphorylation sites. Rapid Commun Mass Spectrom *19*, 57-71.

Gruhler, A., Olsen, J. V., Mohammed, S., Mortensen, P., Faergeman, N. J., Mann, M., and Jensen, O. N. (2005). Quantitative phosphoproteomics applied to the yeast pheromone signaling pathway. Mol Cell Proteomics *4*, 310-327.

Posewitz, M. C., and Tempst, P. (1999). Immobilized gallium(III) affinity chromatography of phosphopeptides. Anal Chem *71*, 2883-2892.

Thingholm, T. E., Larsen, M. R., Ingrell, C. R., Kassem, M., and Jensen, O. N. (2008). TiO(2)-based phosphoproteomic analysis of the plasma membrane and the effects of phosphatase inhibitor treatment. J Proteome Res *7*, 3304-3313.

Xu, C., Inokuma, M. S., Denham, J., Golds, K., Kundu, P., Gold, J. D., and Carpenter, M. K. (2001). Feeder-free growth of undifferentiated human embryonic stem cells. Nat Biotechnol *19*, 971-974.

Yao, S., Chen, S., Clark, J., Hao, E., Beattie, G. M., Hayek, A., and Ding, S. (2006). Long-term self-renewal and directed differentiation of human embryonic stem cells in chemically defined conditions. Proc Natl Acad Sci U S A *103*, 6907-6912.